

Figure 8-11. Taronga - Normalised TFMMR, H_N .

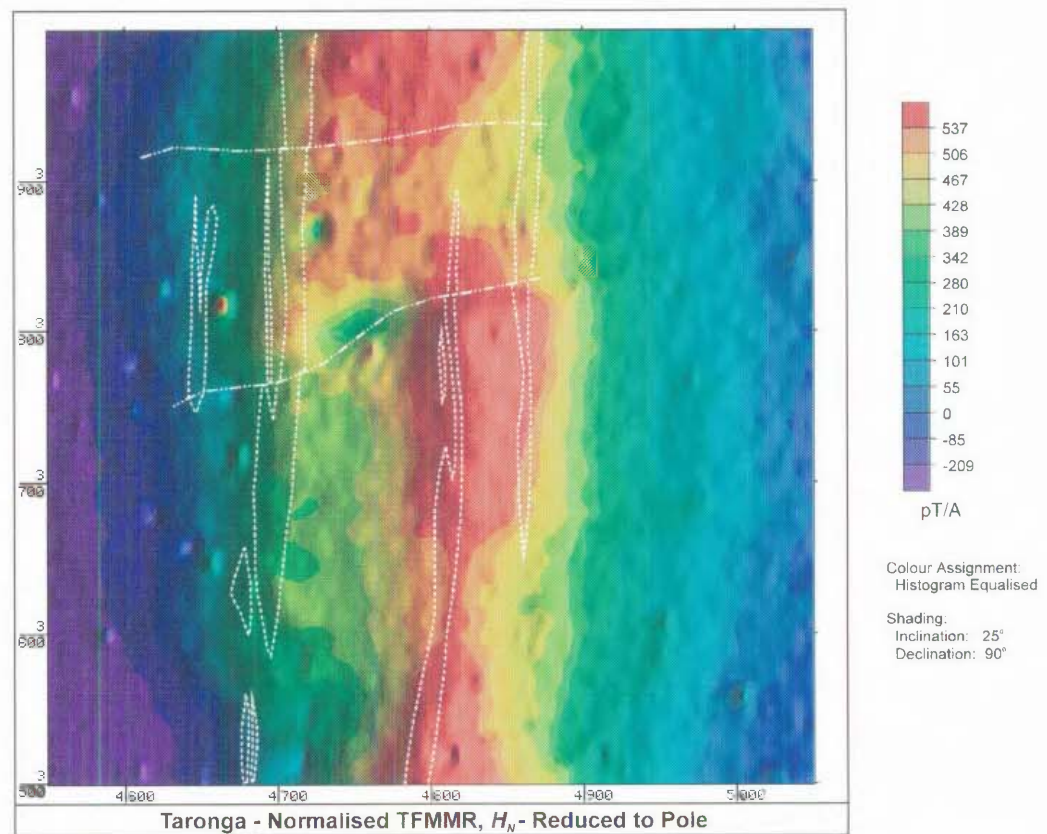


Figure 8-12. Taronga - Normalised TFMMR, H_N , Reduced to Pole.

8.2.5.3 Total Field Magnetometric Induced Polarisation (TFMMIP)

As described in Chapter 7, an induced polarisation response should be detectable as a phase lag between the transmitted current and the received waveform. The received signal is the vector sum of the magnetic field due to current flow in the ground, H_G , and the Primary field, $H_{Primary}$, due to current flowing in the wire feeding the electrodes. Therefore, the calculated phase will be affected by the amplitude of the Primary field as well as the amplitude of the Ground field. With knowledge of the theoretical phase and amplitude of the Primary field, the phase may be corrected using the simple trigonometric relationships previously described.

The corrected phase data was found to be extremely noisy which had the effect of masking any diagnostic information which may have been in the data. Consequently, the phase data were heavily filtered. The filtered, corrected phase, calculated for the fundamental frequency, is shown in Figure 8-14.

The image shows a broad, relative “low” or phase lag in the centre of the grid, flanked by a moderate relative “high” to the east and a strong linear feature to the west. The low corresponds to the general location of the mineralisation. However, there was no suggestion in the images that the individual vein swarms were detected by the parameter. The data range in the image was approximately 40 mrad.

The “high” at the western edge of the grid aroused interest in that the linear feature was effectively in-phase with the transmitted signal and was suspected as being a processing artefact. Close investigation of this feature revealed the fact that the Ground field, H_G , approached zero amplitude in this region, probably because of the very resistive unit to the west of the mineralisation. This posed problems for the phase correction as the data were dominated by the Primary field, $H_{Primary}$, which resulted in a significant “high” or in-phase response. As would be expected, the determination of a phase response was not possible without a Ground field signal. The data in this area were, consequently, considered invalid.

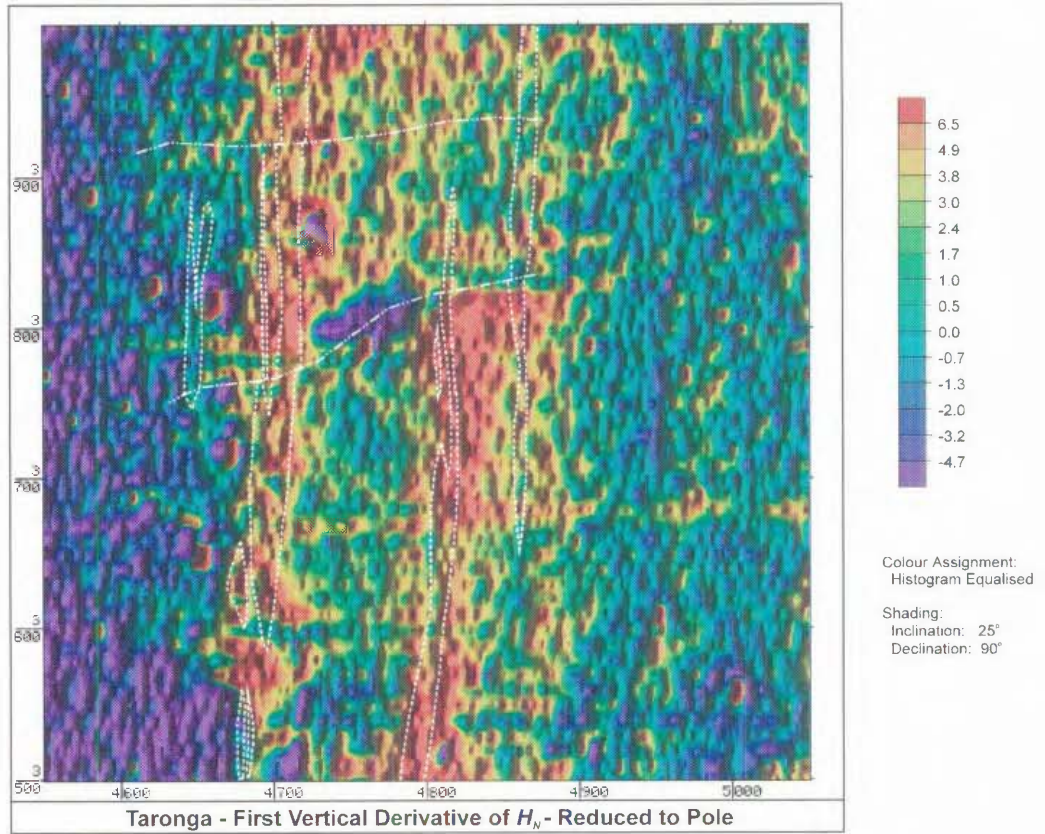


Figure 8-13. Taronga - First Vertical Derivative of H_N - Reduced to Pole.

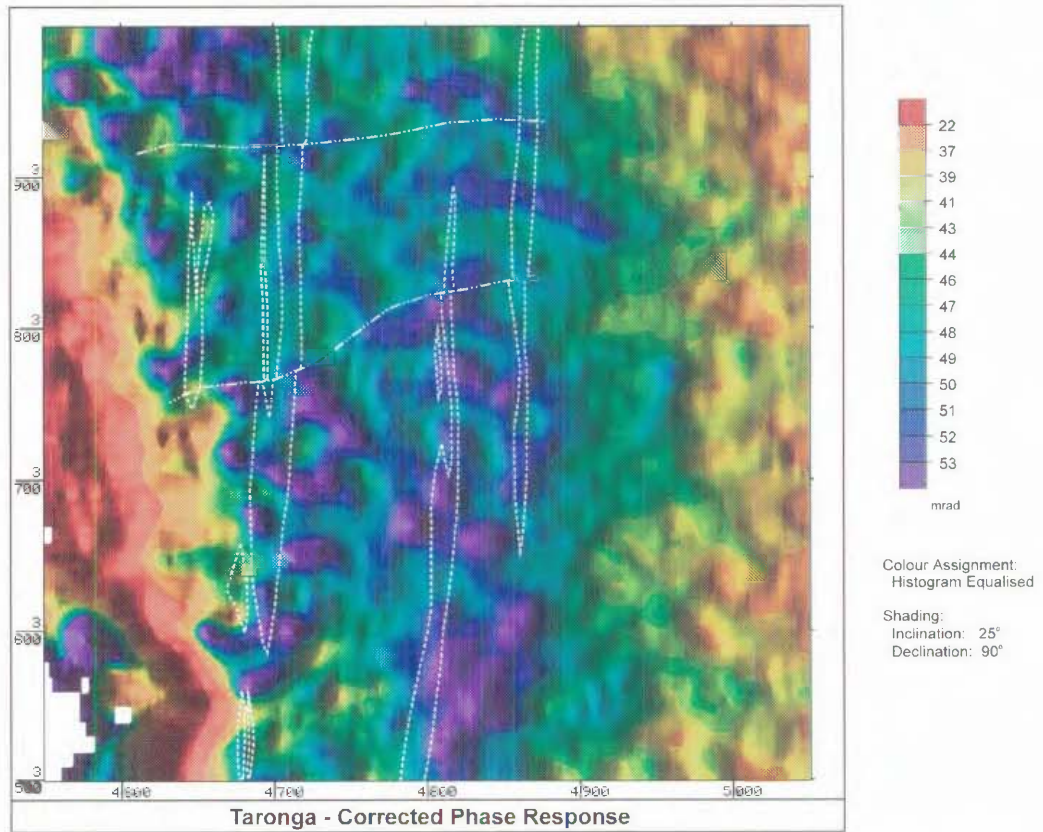


Figure 8-14. Taronga - Corrected Phase Response.

8.2.6 The Effect of Topography on Primary Field Corrections

In all prior surveys, the topography was relatively flat and Primary corrections did not take into account the relative elevations of the current-carrying wire and the survey area. That is, it was assumed that the wire and the survey area were in one plane. However, at Taronga, the total topographic relief exceeded 100 m and it was suspected that variation in topography may have had an effect on the correction for the Primary field.

The calculation of the Primary field was discussed in Section 3.3.1. In summary, the magnetic field due to current flowing in a long straight wire is proportional to the current and inversely proportional to the distance away from the wire. Figure 8-15 illustrates how the magnitude and the direction of the Primary field changes due to variations in the elevation of the measuring point with respect to the wire. W is the location of a long straight wire whose current is flowing out of the page toward the reader. The magnetic field lines are circles with the wire at their centre. By the Right Hand Rule, the direction of the magnetic field produced by current flow is determined to be anti-clockwise.

If P is a measurement point in the same plane as the wire, it can be seen that the direction of the magnetic field at that point is vertical. P' is a point which is the same horizontal distance from W as P but is elevated by a height h relative to W . The effect of elevation is two-fold. Because the distance of P' from W is greater than the distance from P to W , the strength of the magnetic field at P' is reduced compared to that at P . In addition, the direction of the magnetic field changes from vertical by the angle θ . This may serve to increase or decrease the total field measurement depending on the direction of the ambient magnetic field.

The effect of elevation on Primary field corrections is dependent on the angle θ between the horizontal and the line joining the wire and the measuring point. That angle is governed by the elevation of the measurement point relative to the wire as well as its horizontal distance from the wire. It can be seen from Figure 8-15 that if the wire were moved further from the measurement point to the location W_1 thereby reducing the angle θ to θ_1 , then the magnitude of the magnetic field at the measurement point P'

will be reduced as will the change in the direction of the magnetic field vector. Clearly, the effect of topography on Primary field corrections will be lessened, the further the current-carrying wire is kept away from the survey area.

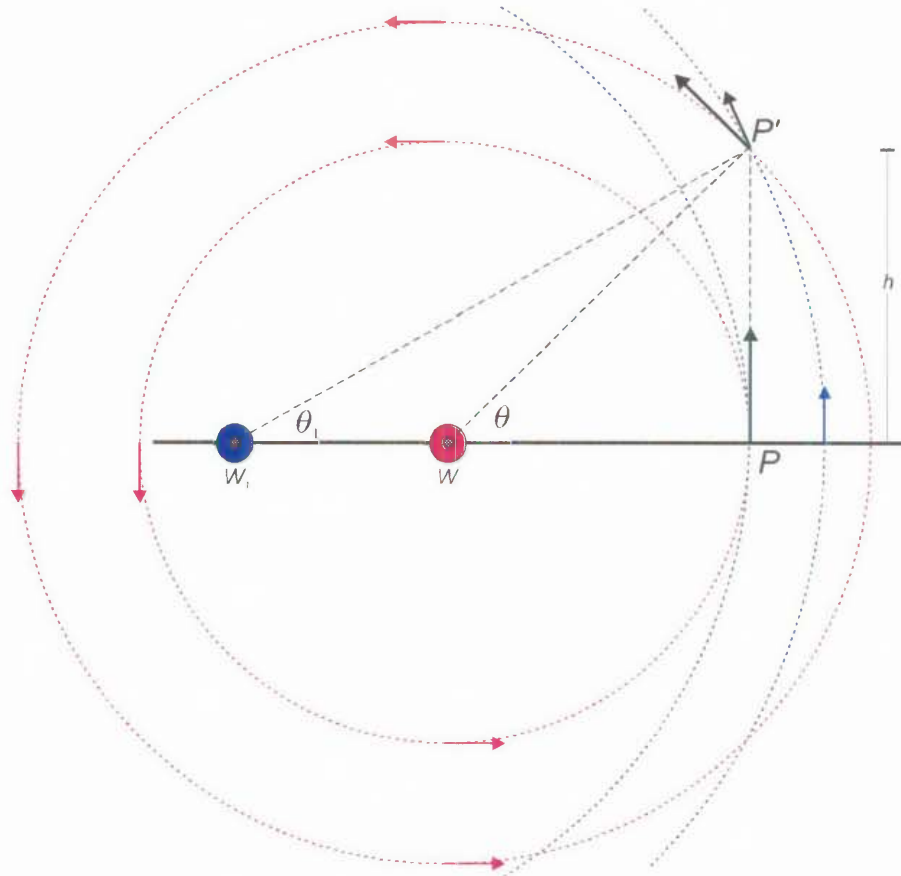


Figure 8-15. Diagram illustrating the effect of elevation on the strength and direction of the magnetic field due to current flowing in a long straight wire.

To examine the effect of topography on Primary field corrections at Taronga, the Primary field was calculated with and without taking relative elevation into account. The difference between the grids was obtained by subtracting the grid with elevation corrections from the grid which was corrected assuming no topographic variation. A colour image showing the result is shown in Figure 8-16.

As expected, the image largely reflects the topography, with the amplitude of the differences increasing towards the current-carrying wire which was laid out to the east of the survey area. The impact of topography on the Primary correction can be observed by correcting the TFM MR data with no elevation correction. The result of this is shown in Figure 8-17. Comparison of the image with that shown in Figure 8-11,

revealed that the main features in the data were still evident. It was concluded that, for the Taronga data, the topographic correction was beneficial, but not critical to the interpretation.

8.2.7 Discussion

As expected, the magnetics component of the SAM data has shown no evidence of the mineralisation directly. However, it may have mapped underlying geological structures which were responsible for emplacement of the mineralisation. The TFMMR data has clearly defined a broad conductive zone and, unlike conventional IP/resistivity techniques, has resolved the individual vein swarms of the Southern Zone mineralisation. The TFMMR anomaly was relatively long wavelength for the line spacing (10 m) used for the survey. Consequently, the line spacing was considered to be oversampling the anomaly.

This survey was a first attempt at extracting IP information with the SAMCard option. Although confidence in the parameter will only be achieved with experience, the image gives some encouragement that IP effects may be detectable with the technique. The TFMMIP parameter has been found to be adversely affected by the influence of the Primary field which requires corrections to be made to the data. It is suggested that the possibility of using time domain waveforms should be investigated. This would enable the determination of parameters related to IP decays in the absence of the Primary field.

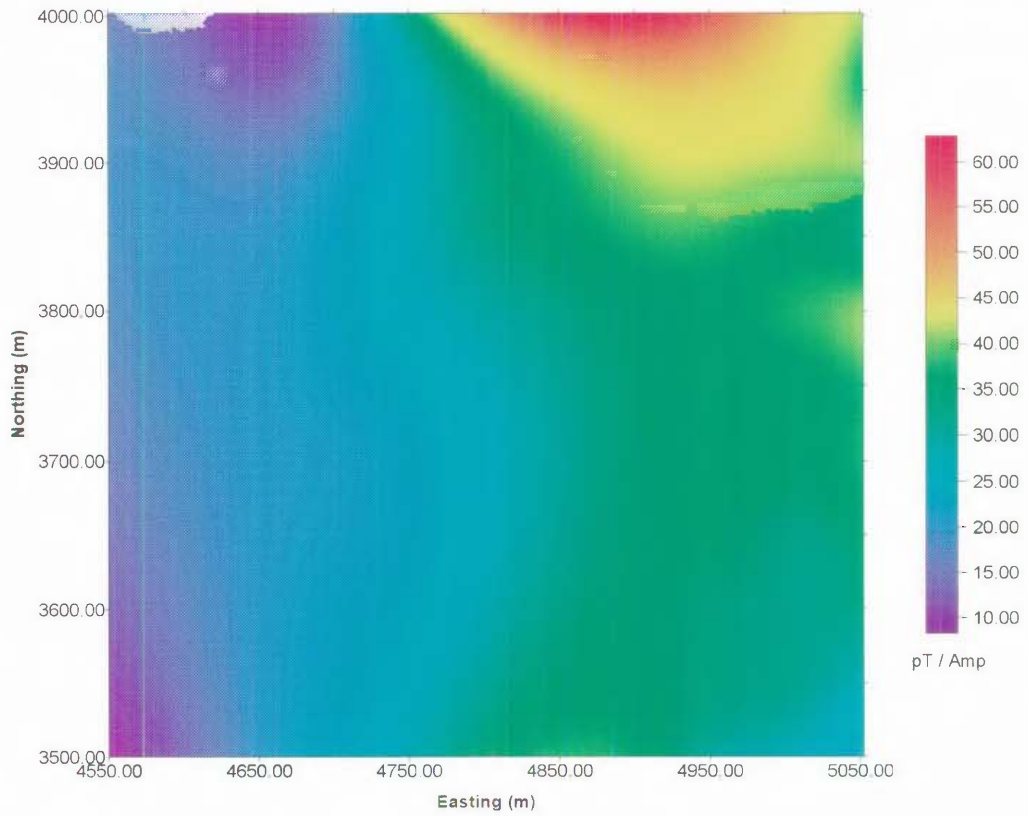


Figure 8-16. The difference in the Primary correction calculated with and without consideration of elevation.

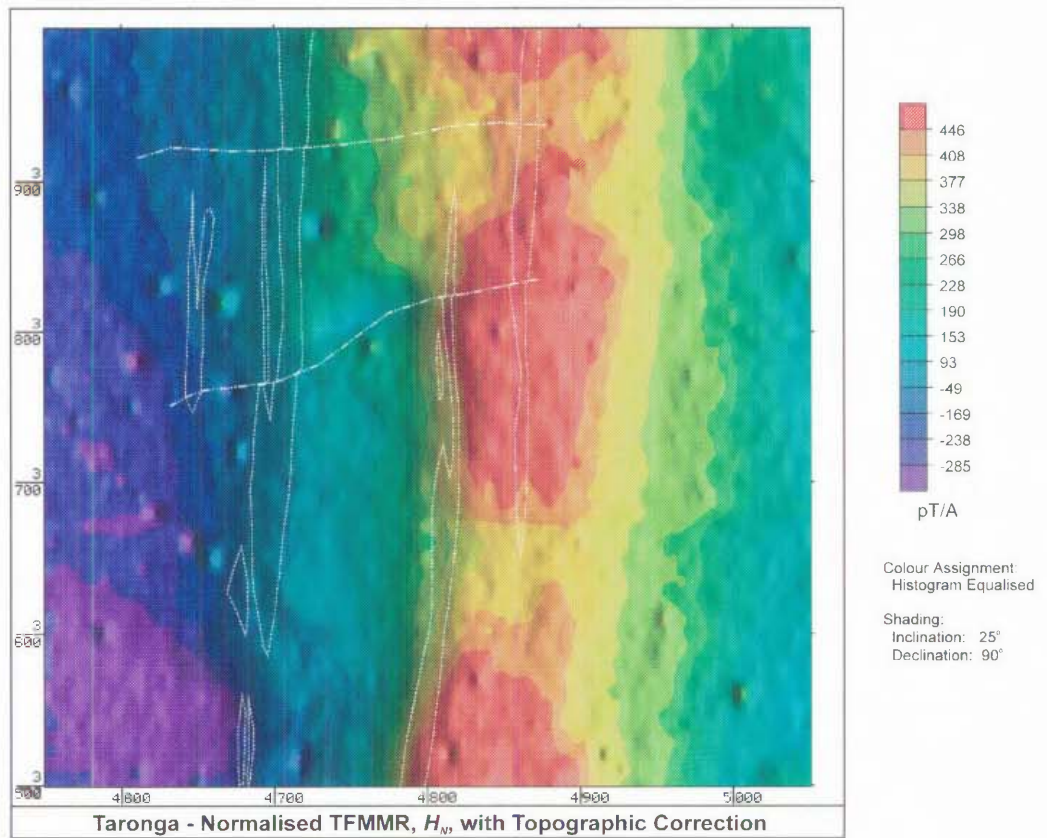


Figure 8-17. TFMMR corrected for the Primary field with topographic correction.

8.3 Case Study #2 - HYC Deposit, McArthur River, Northern Territory

8.3.1 Location

The first reports of mineralisation in the McArthur River district occurred around 1880, with galena veins being noted in carbonate sediments in the area. Exploration in the area was sporadic until 1954, when Mount Isa Mines initiated a general search for guides to exploration for base metals. It was observed that the orebodies of many major base metal fields were of the bedded type and usually occurred at one or two stratigraphic horizons, a fact which was used as an exploration guide.

The exploration strategy proved fruitful and the HYC (Here's Your Chance) silver-lead-zinc deposit was found near the McArthur River, NT in 1955. It is described as

“a sediment-hosted stratiform sulphide deposit which was discovered from drilling under a small, zinc-rich, siliceous dolomite outcrop containing white crystals of hemimorphite” (Hishida *et al.* 1993).

According to Logan *et al.* (1990), the resource is estimated to contain 227 Mt, grading 9.2% Zn, 4.1% Pb, 41 g/t Ag and 0.2% Cu. In recent years, the site has seen considerable infrastructure development and mining of the deposit has recently commenced.

The HYC deposit is situated in the McArthur River area which is located about 590 km northwest of Mt. Isa, Queensland (Latitude: 16°26'S; Longitude: 136°06'E). A location map showing the surface geology for the area is shown in Figure 8-18.

In May/June 1995, a trial Sub-Audio Magnetics survey was conducted at the site in order to determine the applicability of the technique for the detection of the HYC style mineralisation. A specific objective of the trial was to compare the results with those previously published for the MIP technique (Hishida *et al.*, 1993).

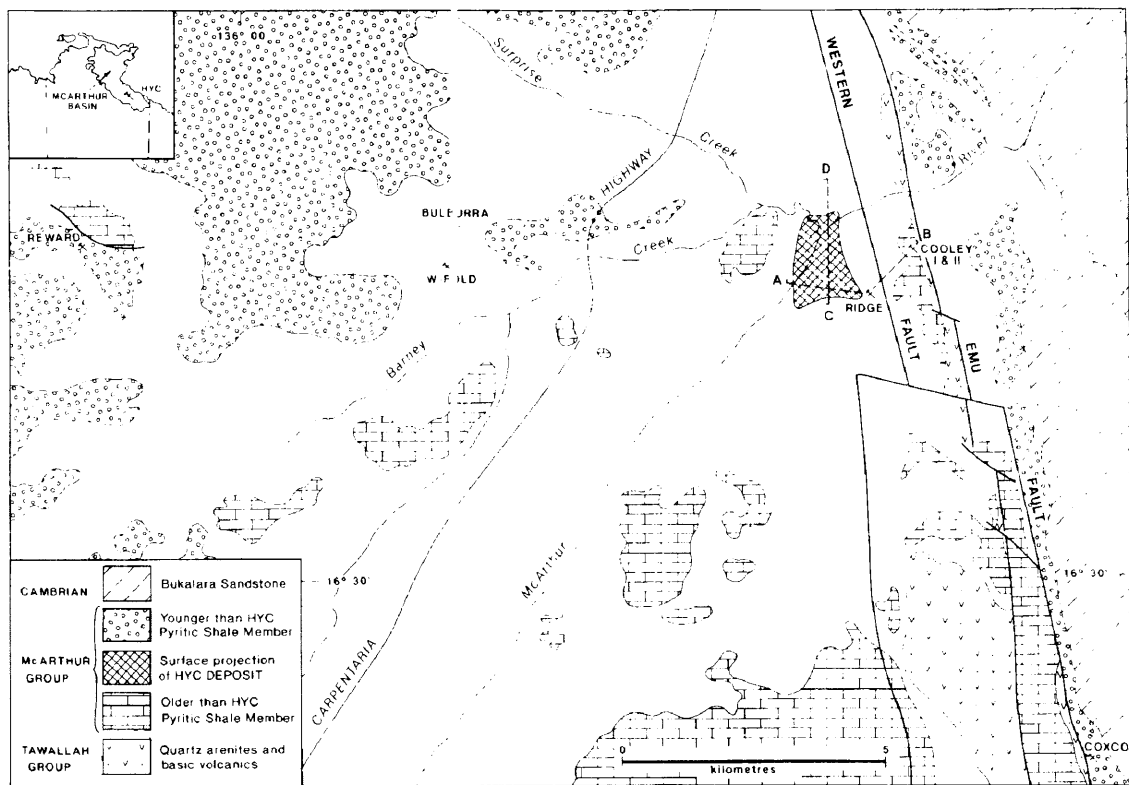


Figure 8-18 Location and Geological Map of the Eastern Batten Trough in the McArthur River Area. Hatched area is surface projection of the HYC deposit. (After Logan *et al.* 1990).

8.3.2 Geological Setting

The geology of the HYC Deposit is described by Logan *et al.* (1990). The orebodies lie in the Batten Trough and are hosted by the Middle Proterozoic McArthur Formation, a north-west trending, intracratonic basin. The sediments comprise from top to bottom, the Tawallah Group (quartz arsenites and basic volcanics), the McArthur Group (mainly carbonates), the Nathan Group (carbonates and arsenites) and the Roper Group (quartz arsenite and micaceous lutites). The McArthur Group which hosts the HYC deposit is composed of a sequence of interbedded dolostone, red beds and quartz arenite, with minor lutite, sedimentary breccia, siltstone and tuff (Logan *et al.*, 1990). The area is bounded to the east by the Emu Fault.

The main orebody is a fine-grained, stratified silver-lead-zinc deposit, situated at the base of the HYC pyritic shale-siltstone member. The deposit covers a total area of about 2 km². It extends 1 km east-west with a shallow easterly dip. Strike length is 1.5 km north-south. The average thickness of the ore horizon is 55 m. The body lies

beneath a black soil plain. The ore itself does not outcrop. The western edge of the orebody is folded and eroded. At its eastern edge, the body interfingers with dolomite at a depth of about 400 m. Smaller coarse-grained deposits of disseminated sulphide occur in the Cooley Dolomite and Emmerugga Dolomite (Williams, 1978). A geological cross-section of the McArthur River area is included as Figure 8-19.

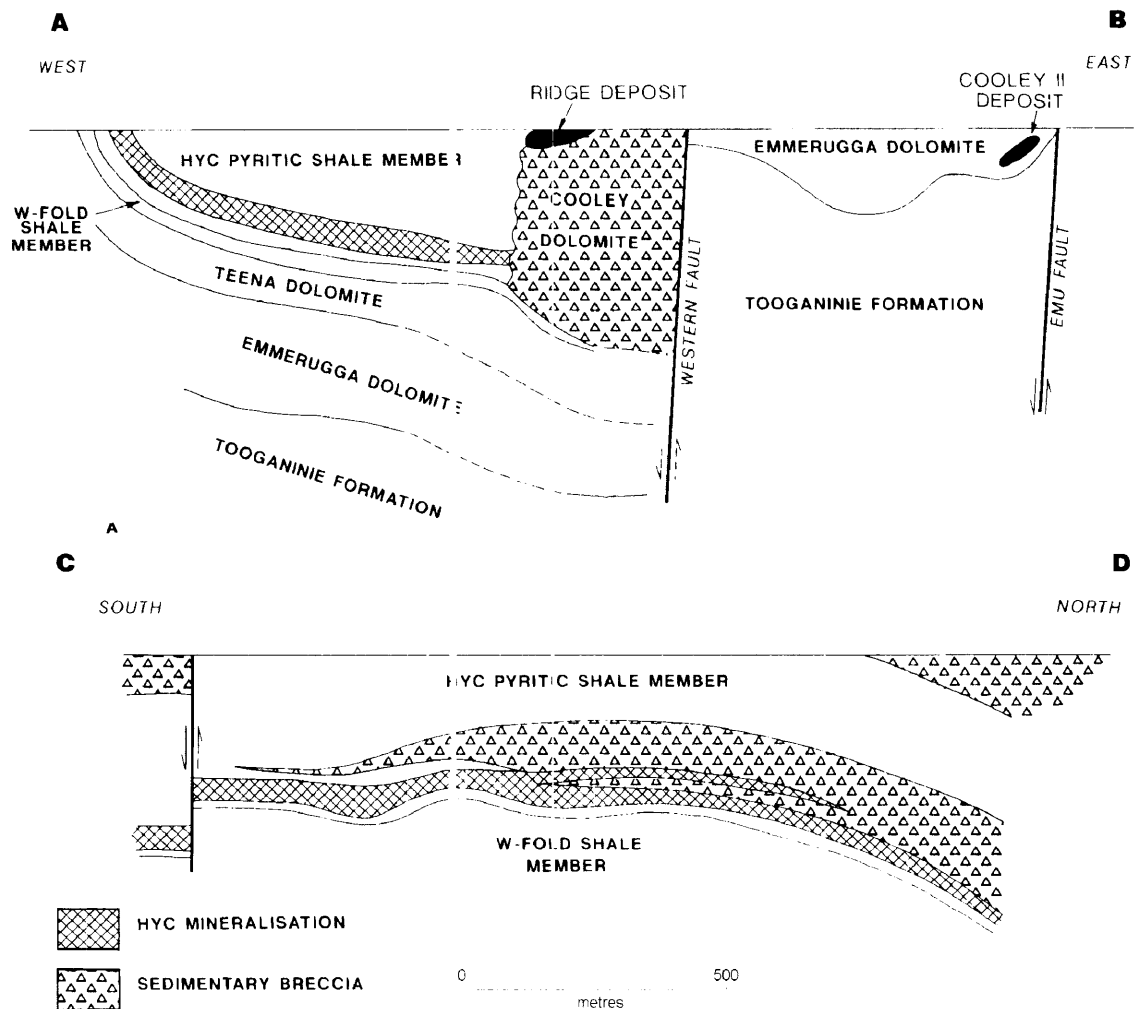


Figure 8-19. Geological cross-sections looking north (Profile A-B) and looking west (Profile C-D) through the HYC deposit (After Logan *et al.* 1990).

8.3.2.1 Mineralisation

The mineralised interval has been divided into seven orebodies which are separated by relatively barren sedimentary breccia and siltstone. The major sulphides are described by Croxford and Jephcott (1972) and Logan (1979) as including two generations of pyrite, sphalerite and galena, with minor chalcopyrite, arsenopyrite and marcasite.

“Pyrite occurs as euhedral to rounded grains up to about 20 μm , and is often bedded or framboidal. Sphalerite and galena occur as laminae or disseminated grains, which in more pyritic areas form the matrix to the pyrite. Chalcopyrite occurs as inclusions in sphalerite, while the other sulphides form isolated grains and minor late stage, crosscutting veins. Discrete silver minerals, with the exception of a small area of tetrahedrite-galena-chalcopyrite mineralisation in the northern section of the lower parts of the deposit, have not been identified.

*There is an overlapping zoning of metals from copper to lead to zinc to iron from north to south in the lower parts of the deposit, and from east to west in the upper parts. The non-sulphide minerals outline a mineral halo in the hanging wall sediments which is recognised by changes from potassium feldspar to albite, and from dolomite to calcite, with increasing distance from the mineralisation” (Lozan *et al.* 1990, 908).*

Apart from the fine grained stratiform HYC deposit, the region also hosts minor, discordant and coarse-grained copper, lead and zinc mineralisation in several locations.

8.3.3 Prior Geophysics

An overview of the geophysics which has been applied to the HYC prospect is presented by Shalley and Harvey (1992). In summary, gravity techniques are complicated by structure and carbonate rocks. Recent EM techniques have provided excellent results in both profiling and sounding modes. GEOTEM and Questem airborne systems both produce clear anomalies over the deposit. The HYC deposit has no magnetic signature, although regional scale magnetics has proven useful in delineating structure.

Of relevance to this thesis, frequency domain MIP trials described by Hishida *et al.* (1993) were conducted in 1992 in order to define the MIP response over the deposit and to compare the results with other geophysical data. The survey was performed over the southern half of the deposit and extended approximately 400 m off the southern edge of the orebody to provide background data. Four contiguous 600 m square grids were surveyed. The locations of the grids with respect to the orebody are shown in Figure 8-3. The surveys employed a transmitter frequency of 1.0 Hz. Survey lines were orientated east-west with 100 m separation. The station spacing was 50 m.

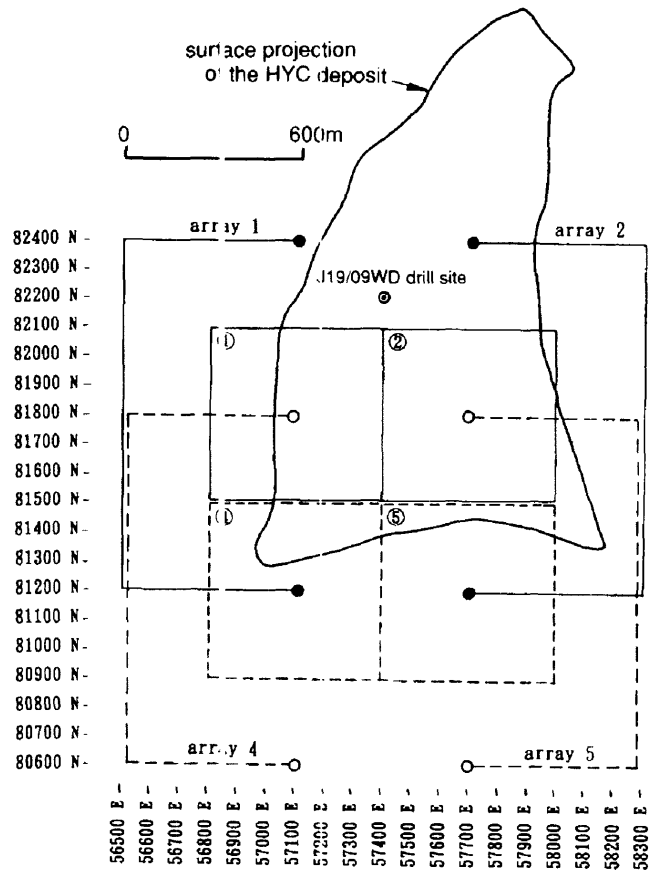


Figure 8-20. Electrodes and cable configurations of the MIP survey over the HYC deposit (After Hishida *et al.*, 1993).

Contours of both normalised horizontal magnetic field, H_N , and relative phase shift (RPS) are shown in Figure 8-21 and Figure 8-22, respectively. The procedure used to merge the four H_N grids is described as follows:

“With H_N , which is a relative measurement, there was almost a constant shift between the eastern arrays (2 and 5) and the western pair (1 and 4), due to H_N increasing west to east. To merge the arrays, 40% was added to all the values of arrays 2 and 5, and the average values were used” Hishida *et al.* (1990, 580).

The H_N values showed a distinct north-south trend and increased strongly from west to east which was interpreted as being due mainly to the HYC deposit and the thickening of the upper pyritic shale-siltstone member. A well-defined linear contact correlated with the western boundary of the HYC deposit, suggesting a strong resistivity contrast between the upper pyritic shale-siltstone member including the HYC ore horizon and the underlying dolomite. A more conductive area in the northeast corner was

interpreted as suggesting thicker or more conductive pyritic shale-siltstone and/or black soil. A “discontinuity” along 81500 mN was interpreted as being due to resistive, possibly dolomitic, plugs.

The RPS, representing the strength of the MIP anomaly, was greater than 0.5° over western half of the deposit but decreased eastward toward the eastern boundary of the deposit where it dropped off rapidly. This highly anomalous response was interpreted as indicating an eastward dipping body correlating well with the known mineralisation.

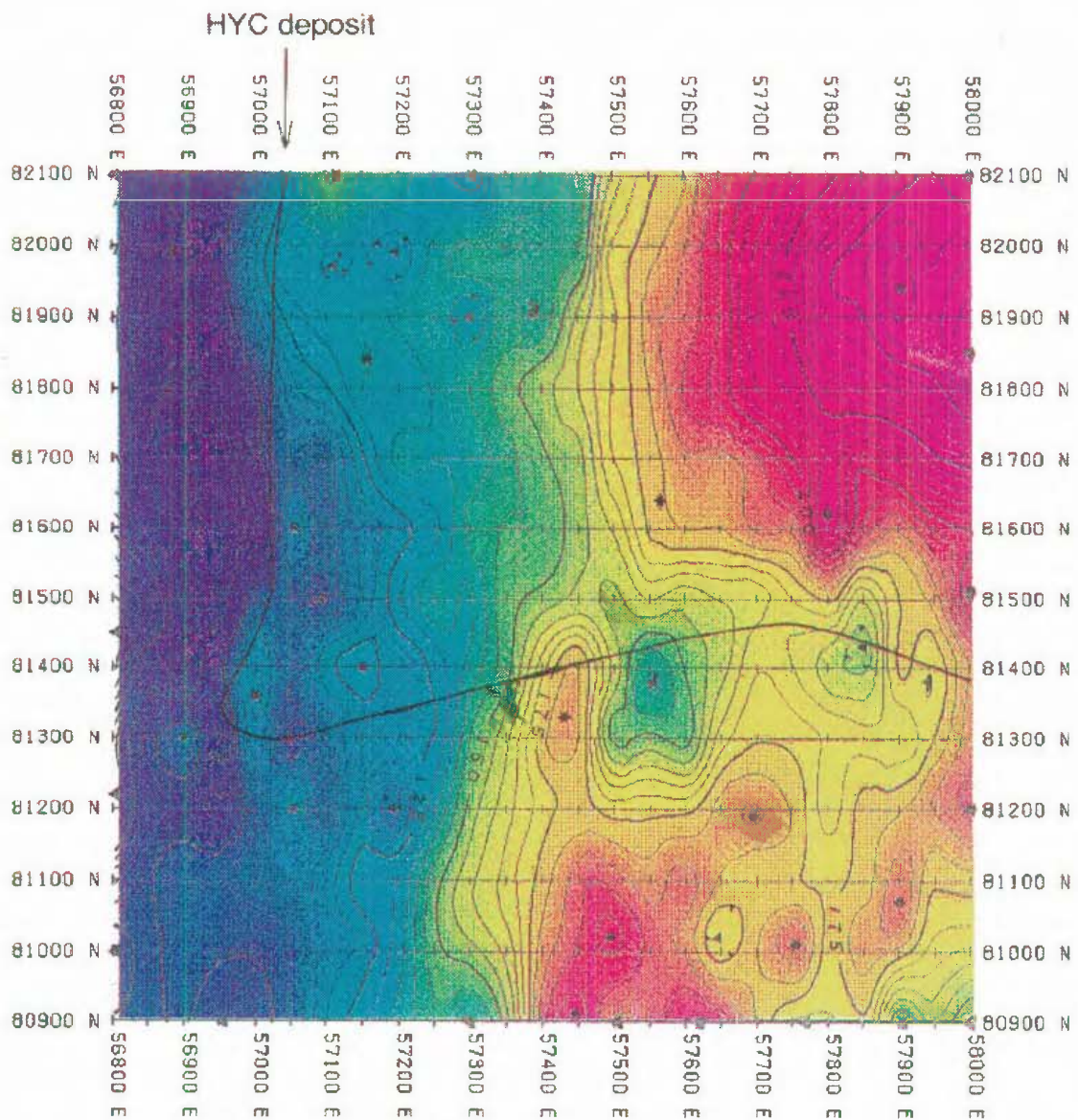


Figure 8-21. Normalised horizontal magnetic field (H_N) contours (%) for current flow parallel to strike over the HYC deposit (After Hishida *et al.*, 1993).

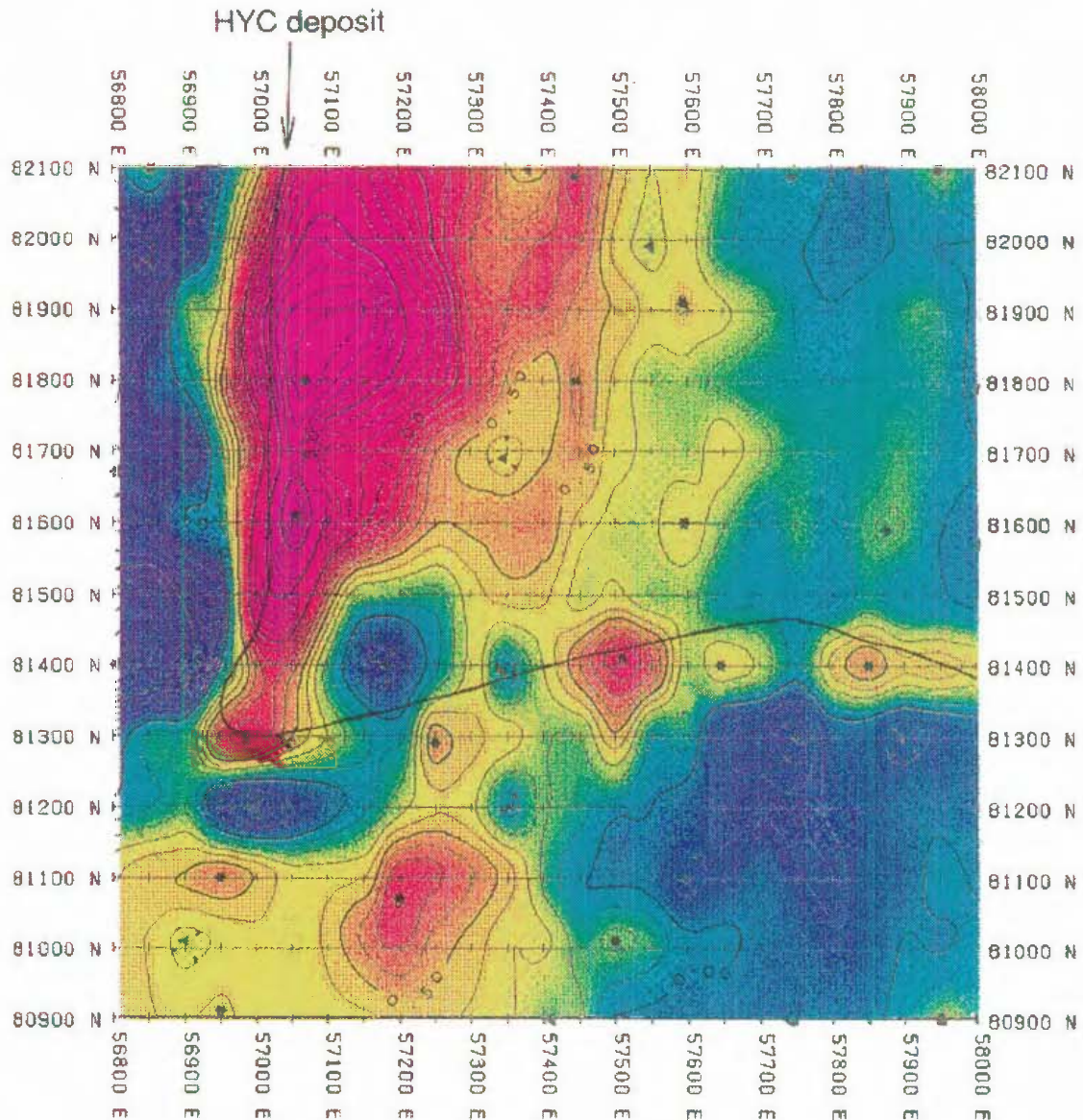


Figure 8-22. Relative Phase Shift (RPS) contours ($^{\circ}$) for current flow parallel to strike over the HYC deposit (After Hishida *et al.*, 1993).

8.3.4 SAM Field Procedure

A single 1.2 km x 1.2 km SAM grid was surveyed at the HYC site. The boundaries of the survey area were defined as shown in Figure 8-23. The survey area was selected so as to coincide with the total area surveyed by Hishida *et al.* (1993). However, a major difference did exist between the surveys. The MIP surveys were conducted by surveying four 600 m square grids. This would have the advantage of greater current densities during the surveys. The main logistical disadvantages would have been the requirement to establish 4 sets of electrodes. From a data processing point of view, the

greatest problem would have been the requirement to append the results, a sometimes difficult task with MMR/MIP surveys (and SAM surveys).

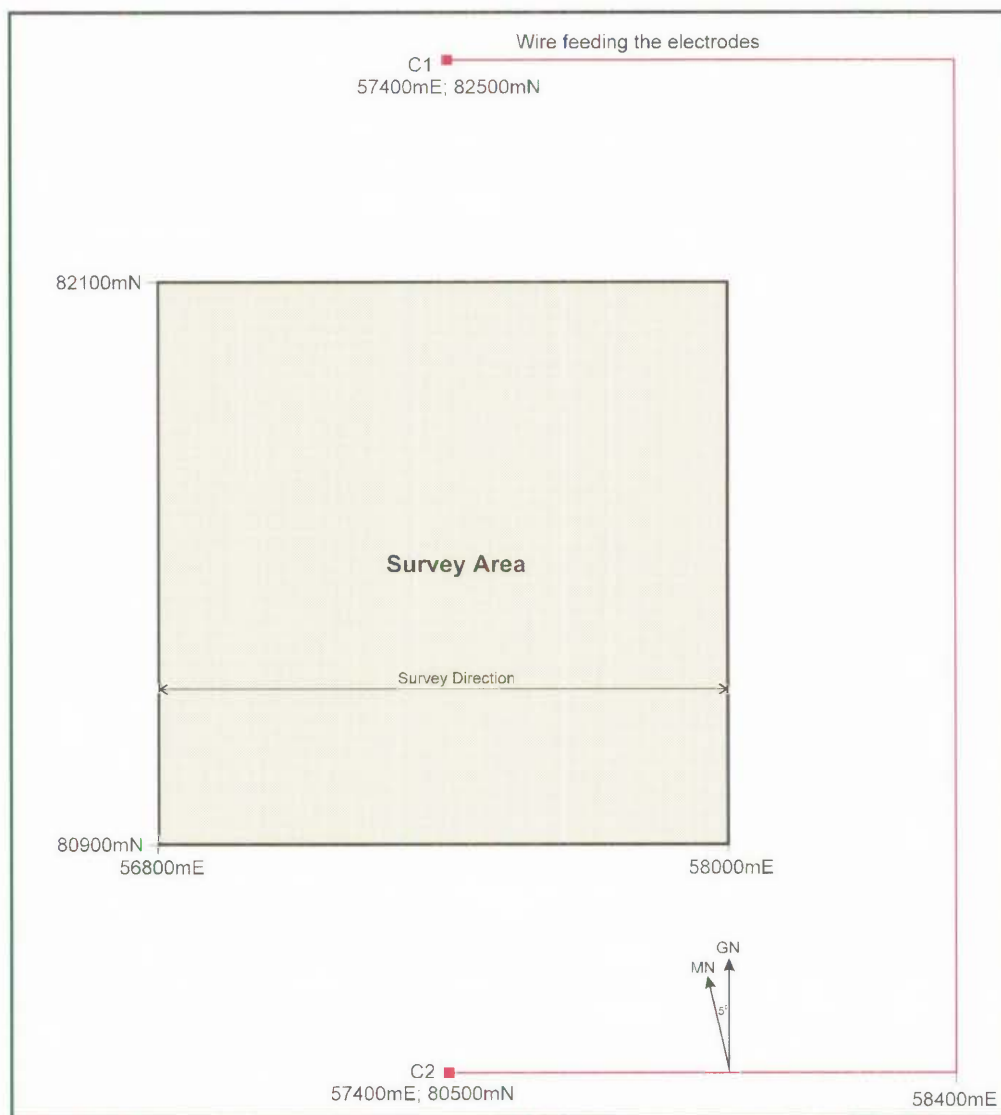


Figure 8-23. Schematic showing the layout of the electrodes and current carrying wire with respect to the survey area.

Electrodes were emplaced at 57400 mE; 82500 mN (C1) and 57400 mE; 80500 mN (C2). The electrodes consisted of buried sheets of aluminium foil. Water and salt were added to the electrodes to improve electrical coupling. Three electrodes approximately 1 m² in area were established at each end of the grid. The wire feeding the electrodes was laid out to the east of the survey area as shown in Figure 8-23. In previous surveys, the wire had been laid out at a minimum distance of 200 m from the survey area. At HYC, that distance was increased to 400 m to further reduce the influence of the Primary field on the recorded waveform.